minerals

MDPI

Article

Recovering Iron Concentrate from Low-Grade Siderite Tailings Based on the Process Mineralogy Characteristics

He Wan [1,2,*], Peng Yi [1], Saija Luukkanen [2], Juanping Qu [1], Chonghui Zhang [1], Shenghong Yang [2] and Xianzhong Bu [1,*]

[1] School of Resources Engineering, Xi'an University of Architecture and Technology, Xi'an 710055, China; yipeng@xauat.edu.cn (P.Y.); qjp@live.xauat.edu.cn (J.Q.); zhangchonghui@xauat.edu.cn (C.Z.)
[2] Oulu Mining School, University of Oulu, 90570 Oulu, Finland; saija.luukkanen@oulu.fi (S.L.); shenghong.yang@oulu.fi (S.Y.)
* Correspondence: wanhe@xauat.edu.cn (H.W.); buxianzhong@xauat.edu.cn (X.B.); Tel.: +86-029-8220-3408 (H.W. & X.B.)

Abstract: Refractory iron ore is often discarded as tailings. This causes a great waste of iron resources. In this paper, the flash roasting-magnetic separation process was designed by combining the magnetic separation process of magnetite and the process mineralogy of iron tailings. The flash suspension roasting effects with 3–4 s roasting time were evaluated by magnetic separation. The MLA results show that the tailings are ground to a fineness of P90 −75 μm, where the distribution of siderite and M/H in the −75 μm particle size is 85.37% and 92.75%, respectively. Moreover, M/H and siderite are mainly associated with muscovite and quartz. This indicates that regrinding for contiguous bodies of M/H and siderite is beneficial for improving the grade and recovery of iron concentrates. The results of the flash roasting-magnetic separation process show that a mixed iron concentrate containing 60.10% Fe with an iron recovery of 81.13% would be achieved after selective grinding and staged magnetic separation of the roasted ore. The result indicates that the flash suspension roasting effects with 3–4 s roasting time are achievable. The study provides an efficient approach for recovering refractory iron from tailings.

Keywords: discarded iron tailings; low-grade siderite; process mineralogy characteristics

Citation: Wan, H.; Yi, P.; Luukkanen, S.; Qu, J.; Zhang, C.; Yang, S.; Bu, X. Recovering Iron Concentrate from Low-Grade Siderite Tailings Based on the Process Mineralogy Characteristics. *Minerals* **2022**, *12*, 676. https://doi.org/10.3390/min12060676

Academic Editor: Saeed Farrokhpay

Received: 12 May 2022
Accepted: 23 May 2022
Published: 27 May 2022

1. Introduction

Iron ore is one of the essential raw materials for refining iron and steel [1]. It promotes national economic and social development and is irreplaceable and nonrenewable. Iron ore has been added to China's strategic resource list in 2021 [2,3].

China's iron ore resources are relatively abundant, with the world's fourth-largest total reserves [4]. However, more than 97% of the iron ore are low-grade iron ore resources, such as limonite, siderite, and high phosphorus oolitic hematite [5,6]. These ores have the characteristics of low grade, high impurity, fine particle size, and complex composition. It is challenging to recover effectively using conventional beneficiation methods [5,7]. Therefore, for a long time, refractory iron ore is often discarded as tailings due to the limitations of the separation technology and costs [8,9].

Roasting-magnetic separation technology is an effective method for recovering refractory low-grade iron ore [7–9]. First, the magnetization roasting method is used to modify the refractory iron ore, transforming it from a weakly magnetic mineral to a strongly magnetic one, thus increasing the separability of the refractory iron ore.

Temperature is one of the essential parameters for magnetization roasting. Zhang et al. found that, under mildly reducing conditions, the hematite could be reduced to magnetite, and siderite could decompose to magnetite and wustite, the ratio depending on temperature [10]. Their reaction equations are as follows.

$$FeCO_3\ (s) \rightarrow FeO\ (s) + CO_2\ (g) \quad (1)$$

$$FeO\ (s) + 1/3\ CO_2\ (g) \rightarrow 1/3\ Fe_3O_4\ (s) + 1/3\ CO\ (g) \quad (2)$$

$$Fe_2O_3\ (s) + 1/3\ CO\ (g) \rightarrow 2/3\ Fe_3O_4\ (s) + 1/3\ CO_2\ (g) \quad (3)$$

In the magnetization roasting process, reactions 1 and 2 are continuous processes. FeO is the reaction intermediate. The overall reaction 4 for the magnetization roasting process is obtained by combining reactions 1 and 2 [11]. The Gibbs free energy of reactions 3 and 4 are shown in Figure 1.

$$FeCO_3(s) \rightarrow 1/3\ Fe_3O_4\ (s) + 2/3\ CO_2\ (g) + 1/3\ CO\ (g) \quad (4)$$

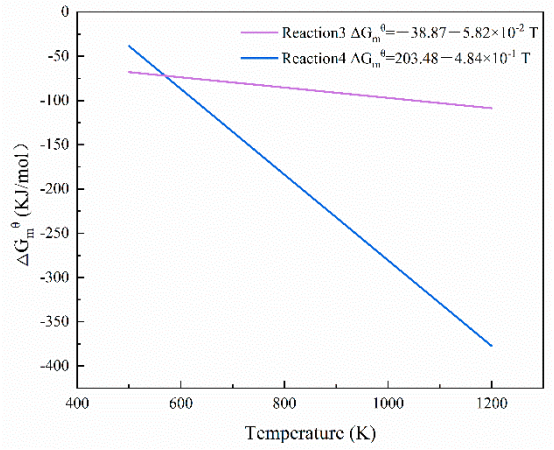

Figure 1. The Gibbs free energy of reactions 3 and 4.

Figure 1 shows that the Gibbs free energy of reactions 3 and 4 are always negative in the range of 400 K to 1200 K [10,11]. Moreover, the higher the roasting temperature, the more easily reaction 3 and 4 occurs. These indicate that during the roasting process reactions 3 and 4 will occur spontaneously at roasting temperatures above 500 K. In addition, the thermodynamic analysis only theoretically evaluates the reaction trend. The reliability of reactions 3 and 4 has been confirmed by the experimental studies of Zhang and Zhang et al. [12,13]. Zhang et al. also found that the rising temperature was favorable for the reaction rate of siderite decomposition and hematite reduction, which would generate magnetite spontaneously [11]. Even the magnetization roasting time for siderite and hematite could be reduced from 340 s at 510 °C to 69 s at 720 °C [14]. Feng et al. have predicted that for Daxigou siderite, at sufficiently fine particle size, the magnetization reaction could be completed within 10 s when temperatures were above 650 °C; at temperatures above 750 °C, the magnetization reaction took less than 1 s [15]. However, studies have not reported on the magnetization roasting time in less than 30 s. This may be because the refractory iron ores that have been studied were rarely ground to the same fineness as Daxigou siderite.

The particle size of the mineral is an important process mineralogy parameter. It also is another essential parameter affecting magnetization roasting [16,17]. Liu et al. found that hematite particle size significantly influenced the magnetization roasting efficiency [18]. During the suspension roasting process, as the particle size was reduced, the rate of conversion of Fe_2O_3 to Fe_3O_4 increased. Gao et al. found that at a fixed time the reduction rate for large particles was less than for small particles because the reduction rate was decreasing with time until complete reduction is achieved [19]. Therefore, finer particle size will be beneficial to increasing the magnetization reaction rate.

The above results indicate that the ore's particle size distribution and intergrowth characteristics determine the process flowsheet and parameters for the suspension roasting-magnetic separation of refractory iron ores. Meanwhile, numerous studies have also shown

that mineralogy research can optimize beneficiation processes and parameters to improve the beneficiation index [20–22].

This paper is the first to recover iron from iron tailings by flash suspension roasting-magnetic separation with a roasting time of 3–4 s. To simplify the flash suspension roasting-magnetic separation experimental process, the mineral liberation analyzer (MLA) was used to conduct process mineralogy research on discarded iron tailings in Shaanxi. The characteristics of particle size distribution, liberation, and intergrowth were identified to estimate roasted ore fineness and rough concentrate regrind fineness by MLA. The flash suspension roasting effects are evaluated by magnetic separation. The reasons for iron concentrate with iron grades ≥60% not being available in previous studies are discussed.

2. Materials and Methods

2.1. Materials

Discarded iron tailings in this study were obtained from Daxigou Mining Company in Shaanxi, China. The chemical multi-element analysis results and mineral compositions of the discarded iron tailings are shown in Table 1 and Figure 2. Table 1 shows the total Fe content in the discarded iron tailings was 20.25%. Figure 2 shows that the iron tailing includes siderite, hematite, magnetite, quartz, muscovite, and kaolinite. The Daxigou iron ore mine is the largest siderite deposit in China. It has a geological reserve of 302 million tons. The siderite and hematite have very fine particle sizes and are intergrown with vein minerals [23].

Table 1. The results of chemical multi-element analysis of the discarded iron tailings.

Component	TFe	Al_2O_3	SiO_2	CaO	MgO	K_2O	P	S	MnO	TiO_2
Content (%)	20.25	15.22	41.45	0.44	1.30	1.30	0.01	0.25	0.80	0.45

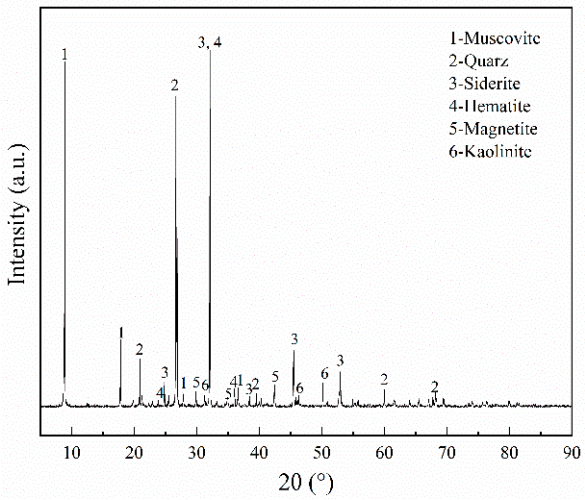

Figure 2. The XRD diffraction results of the discarded iron tailings.

2.2. Process Mineralogy Characteristics

The process mineralogy characteristics were mainly identified via MLA with SEM-EDS (FEI Quanta200-EDAX Genesis XM 2i, FEI Corporation, Hillsboro, OR, USA). The operation and image acquisition of the apparatus was controlled using SEM Control and MLA Investigator software. The optimal operating distance and electron beam acceleration voltage were 10 mm and 25 kV, respectively. During MLA work, differences in the greyscale of backscattered electron images were used to distinguish between different phases; energy spectra were used to identify minerals quickly and accurately, and modern image analysis techniques were used to obtain process mineralogical parameters [22,24–27]. The detailed MLA measurement modes have been reported in the previous literature [24–27].

The following data could be obtained from the MLA: element distribution, particle size distribution, liberation degree, intergrowth relationship, etc.

The mineral composition was analyzed by X-ray diffraction (Shimadzu D/MAX-RA, Shimadzu Corporation, Tokyo, Japan). The operating parameters were: Cu target radiation, nickel filter, tube voltage 40 kV, tube current 40 mA, scanning range 2θ = 5°–90°, step width 0.033°, scanning speed 12°/min, operating temperature 25 °C.

The method of iron phase analysis was from the literature (Figure 3) [11,28]. The chemical composition of iron tailing was analyzed by the potassium dichromate titration method and Inductively Coupled Plasma Mass Spectrometry (ICP-MS, Thermo Fisher Scientific Inc., Waltham, MA, USA).

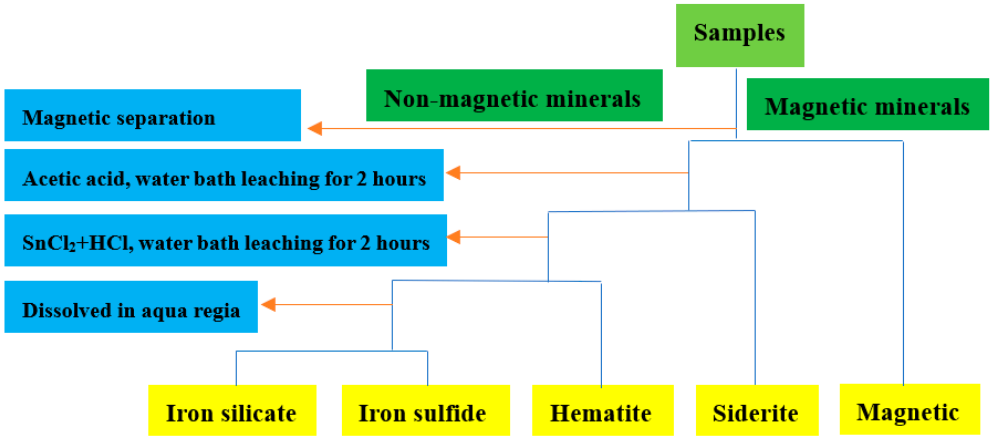

Figure 3. Iron phase analysis.

2.3. Flash Suspension Roasting-Magnetic Separation Procedure

The discarded iron tailings were first ground to 90.0% −75 μm using a dry vertical mill (DL-M-R500, self-developed). Milled tailing was then reduced for 3 s to 4 s at 780 °C with 10% CO in the CO_2 using a suspension roaster (Fluidized bed, DL-R-B01, self-developed). The roasted ore was next prepared into a 30% concentration pulp fed into a wet magnetic separator (DCXJ-400 × 240, Shandong Huatech Magnetics Technology Co., Weifang, China) with 1500 Oe, one rougher concentrate, and one tailing. The rougher concentrate was ground to 94.5% −38 μm using a wet ball mill (XMQ-240 × 90, Jilin Prospecting Machinery Factory, Jilin, China). The mill product was subjected to three sequential magnetic separations in the magnetic separator with 1300 Oe, 1000 Oe, and 700 Oe, and obtained one iron concentrate and three middlings. The last two middlings were combined and ground to 96.0% −38 μm using a wet ball mill (RK/ZQM-150 × 50, Wuhan Rock Grinding Equipment Manufacturing Co., Wuhan, China). The mill product was subjected to 1-time magnetic separations in the magnetic separator with 1500 Oe and obtained one iron concentrate and one middling. The flowchart of flash suspension roasting-magnetic separation is shown in Figure 4. The schematic diagram of the flash suspension reactor is shown in Figure S1 in Supplementary Materials.

2.4. Recovery of Concentrate

The recovery of Fe during the separation was calculated using the equation as follows,

$$\varepsilon = \frac{\beta \times \gamma_\beta}{\alpha \times 100} \times 100\% \quad (5)$$

in which ε is the recovery of Fe during separation, %; α is the grade of Fe in the discarded iron tailings, %; β is the grade of Fe in the concentrate, %; γ_β is the yield of concentrate during separation, %.

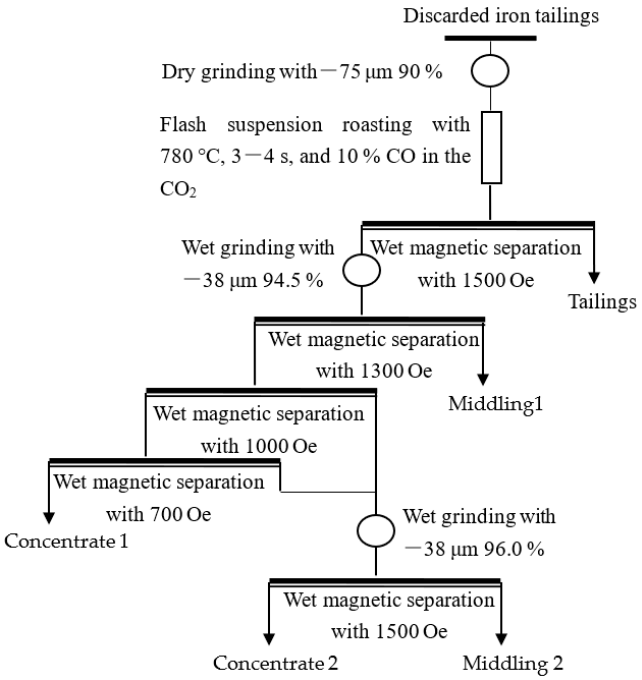

Figure 4. The flowchart of flash suspension roasting-magnetic separation.

3. Results and Discussion

3.1. The Iron Phase Compositions

The results of the iron phase analysis are shown in Table 2.

Table 2. Iron distribution in tailings.

Fe Phase	In Carbonate	In Hematite	In Magnetic Iron	In Silicate	TFe
Content (%)	12.85	5.28	1.60	0.85	20.58
Distribution rate (%)	62.44	25.66	7.77	4.13	100.00

Table 2 shows the content of Fe in carbonate/hematite/magnetic iron/silicate is 12.85%/5.28%/1.60%/0.85%. The distribution rate of Fe in carbonate/hematite/magnetic iron/silicate is 62.44%/25.66%/7.77%/4.13%. Therefore, the maximum theoretical recovery of iron in the tailings is 95.87%.

3.2. Particle Size Distribution Characteristics of Major Iron Minerals

The particle size distribution characteristics of magnetite + hematite (M/H) and siderite in the tailings from the MLA analysis are shown in Figure 3. The statistical result of the particle size distribution are shown in Table 3.

Table 3. The statistical result of particle size distribution.

Particle Size/μm	Siderite (%)		M/H (%)	
	Content	Cumulative Distribution	Content	Cumulative Distribution
+75	4.82	14.63	4.93	7.25
−75~+38	14.56		11.72	
−38~+19	30.9		7.77	
−19~+9.6	23.28		12.55	
−9.6~+4.8	12.81	85.37	26.72	92.75
−4.8~+2.4	3.52		28.72	
−2.4~+1.2	0.27		5.18	
−1.2	0.02		0.1	

Combining the results of Table 3 and Figure 5 found that the particle size of M/H in the tailing is mainly distributed in the size range of −75 μm, accounting for 92.75%, of which −9.6 μm~+4.8 μm and −4.8 μm~+2.4 μm account for 26.72% and 28.72%, respectively. The siderite particle size in tailing is distributed in −75 μm, accounting for 85.37%, with 30.90% in −38 μm~+19 μm and 23.28% in −19 μm~+9.6 μm, which is coarser than M/H. This indicates that M/H is more amenable to grinding than siderite.

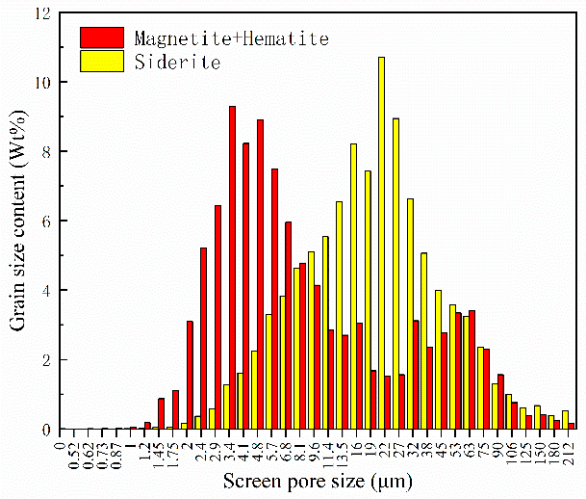

Figure 5. The particle size distribution characteristics of M/H and siderite in the tailing.

3.3. Liberation Degree and Intergrowth Characteristics of Major Iron Minerals

The liberation degree and intergrowth characteristics of major iron minerals are shown in Figure 6.

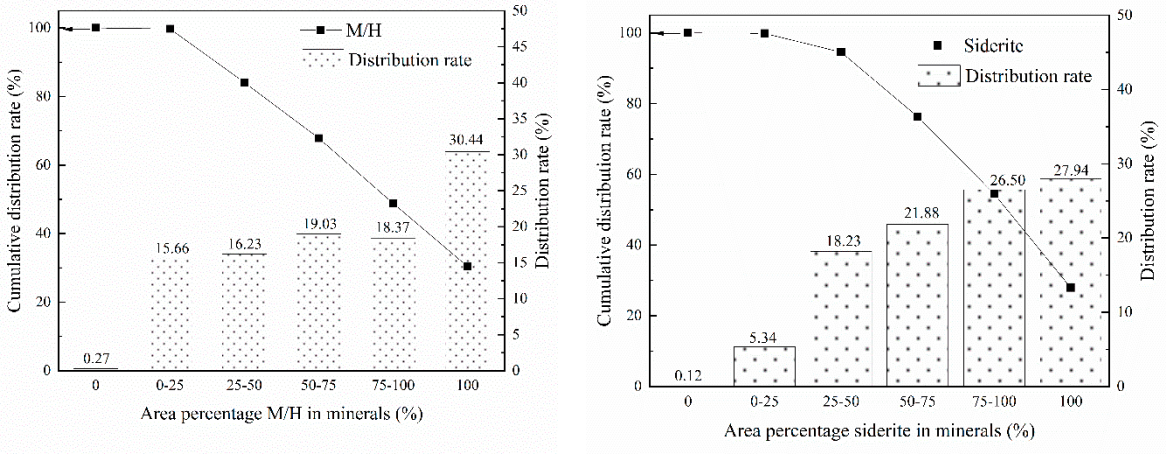

(**a**) (**b**)

Figure 6. Liberation degree of major iron minerals. (**a**) M/H; (**b**) siderite.

Figure 6a shows that the M/H in this tailing has a monomeric dissociation of 30.44% and that a 75–100% exposed area of contiguous bodies as rich intergrowth was 18.37%. The total content of rich intergrowth and monomer was 48.81%. The content of poor intergrowth was over 50%. This indicates that M/H has a low liberation degree. The results in Figure 6b show that the mono-mineral liberation degree of siderite was 27.94%; the total content of rich intergrowth (area percentage, more than 75%) and monomer was 54.43%. The content of poor intergrowth was 45.57%. For magnetic separation, the liberation degree of siderite is more suitable than that of M/H. These results explain the low mono-mineral liberation degree of M/H and siderite in iron tailings under the current grinding fineness.

Their liberation degree can be increased by improving the grinding fineness. However, at a grinding fineness of −75 μm at 90%, the inclusions of both siderite and M/H in the tailings were less than 1%. This can be used for flash magnetization roasting.

Table 3 result shows M/H and siderite have been ground to a fineness of 92.75% and 85.37% with −75 μm, especially M/H, which already has a −9.6 μm content of 60.72%. The siderite has a −9.6 μm content of 16.63%. This indicates that the M/H is being ground too fine at the current grinding fineness to facilitate recovery by magnetic separation [29,30]. However, previous studies have found that with a regrind fineness of −43 μm at 95%, the grade of iron ore concentrate is less than 60% [31]. This indicates that the regrind fineness does not achieve the requirement for monomer dissociation. The regrind fineness needs to be increased. However, high grinding fineness is not favorable for magnetic separation. Therefore, it is necessary to carry out the regrinding of the middlings. This will improve the grade of the iron concentrate while ensuring iron recovery. The regrind fineness was determined to be −38 μm at 94.53% (−43 μm at 95%). The regrind fineness of the congeners was set at −38 μm at 96%.

The mineral map of the tailing is shown in Figure 7. The intergrowth relationship between major gangue minerals and major iron minerals is shown in Figure 8.

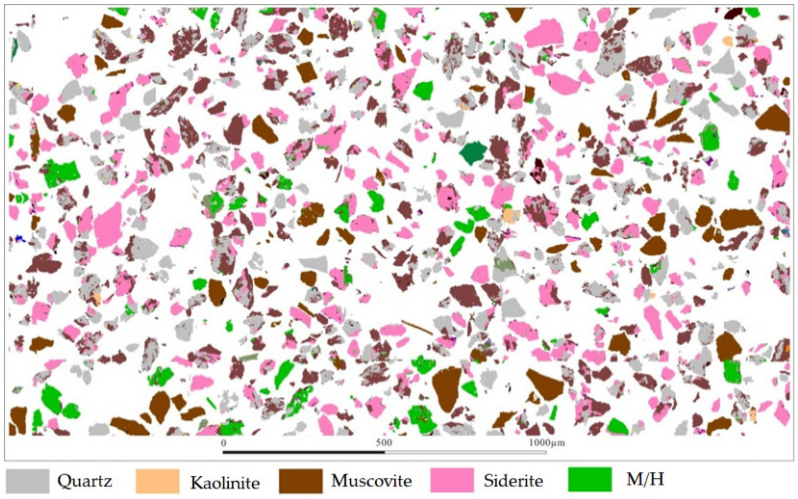

(**a**)

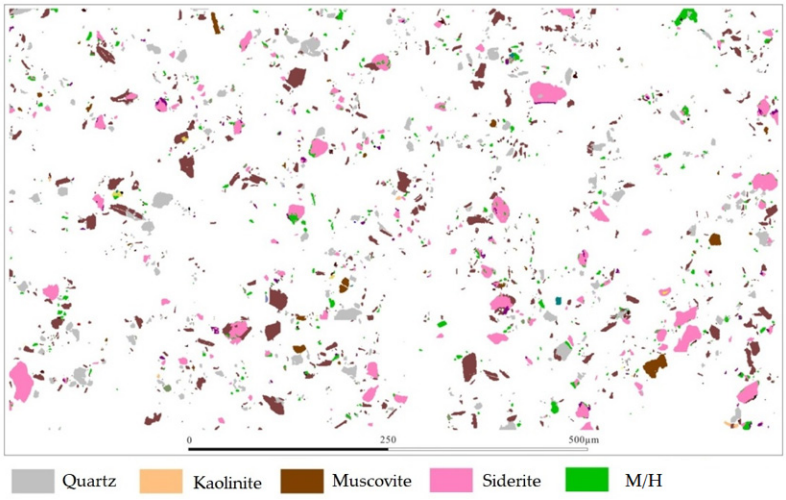

(**b**)

Figure 7. The mineral map of the tailing. (**a**) the particle size of −38~+75 μm and (**b**) particle size of −38 μm.

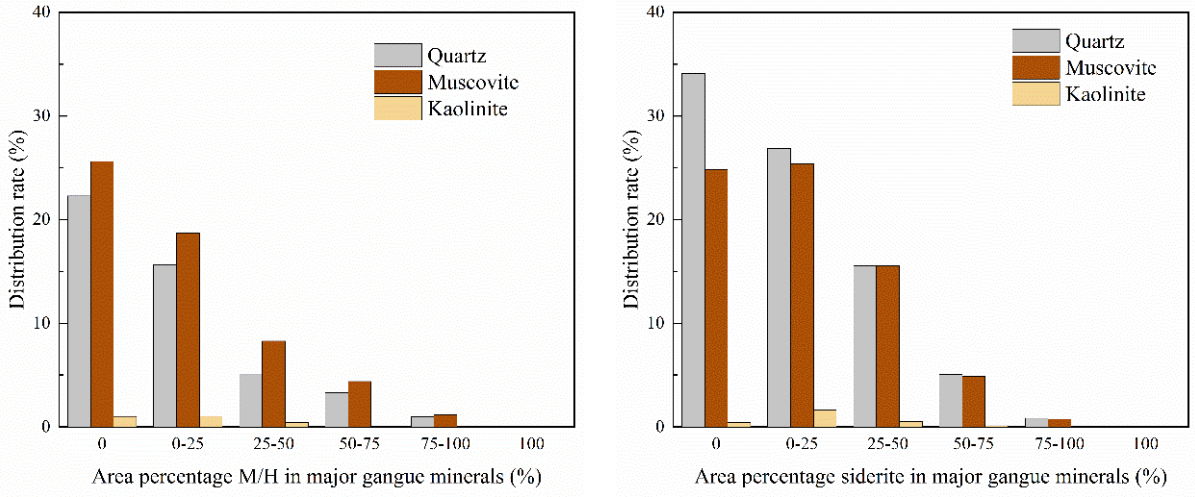

Figure 8. Intergrowth relationship between major gangue mineral and iron minerals (**a**) Intergrowth relationship between major gangue mineral and M/H; (**b**) Intergrowth relationship between major gangue mineral and siderite.

Figures 7 and 8 show that within the non-monolithic M/H and siderite mineral particles, the gangue minerals associated with M/H are quartz, muscovite, and kaolinite. Figure 8a shows that as the exposure of M/H and siderite increases, the area occupied by the major gangue becomes gradually smaller; the major gangues are associated with M/H in the following order: muscovite > quartz > kaolinite; The major gangues are associated with siderite in the following order: muscovite > quartz > kaolinite. These indicate that M/H and siderite are mainly associated with muscovite and quartz. The main impurities in the iron concentrate are likely to be muscovite and quartz. Therefore, selective grinding for contiguous bodies of M/H and siderite is beneficial for improving the grade and recovery of iron concentrates [29].

3.4. Application in Flash Suspension Roasting-Magnetic Separation

The mineralogical information above indicated that the discarded iron tailings were low-grade siderite. The content of impurities such as S and P are low in the tailings. Moreover, they are seldom closely associated with the main iron minerals (M/H and siderite). The effect of impurities (S and P) on the iron concentrate can be disregarded. The main gangue minerals are quartz, muscovite, and kaolinite. Quartz/muscovite is closely associated with siderite/M/H. The current grinding fineness is −75 μm, accounting for 90% of the total. The particle size of M/H in the tailings is mainly distributed in the size range of fewer than 75 μm, accounting for 92.75%, especially the size of −9.6 μm, accounting for 60.72%. This may be detrimental to its recovery by magnetic separation. Siderite is mainly distributed in the particle size range of −75 μm for 85.37%. Only 16.63% of siderite have a size of −9.6 μm. Nearly 85% of the siderite in the particle size can be recovered by magnetic separation. There are significant congeners of quartz and muscovite with major iron minerals at the current grinding fineness. They can affect iron concentrate grades and recoveries [30,32,33]. Therefore, it is necessary to carry out regrinding of intermediate products to improve iron concentrate grade or recovery [29]. The results are shown in Table 4.

Table 4 shows that the iron concentrates 1 and 2 with Fe grade of 60.10% and 60.15% and iron recovery of 73.35% and 7.78% were obtained under the flash suspension roasting-magnetic separation process. A mixed iron concentrate with an iron grade/recovery of 60.10%/81.13% can be obtained. The XRD results of the mixed iron concentrate are shown in Figure 9. The diffraction intensity and content distribution of major iron minerals and gangue minerals in mixed iron concentrate differed significantly from the discarded iron

tailings (Figure 9). The mixed iron concentrate contains magnetite, hematite, quartz, and muscovite. This indicates that despite grinding finenesses to 94.5% −38 μm, there are still massive concretions of quartz and muscovite with iron minerals in the iron concentrate. This will affect the quality of the iron concentrate and is the reason why iron concentrates with iron grades ≥60% were not available in the previous study. Concentrate 2 is obtained from a portion of the middling (grade of 25.58%) by a regrinding-magnetic separation process. This result is consistent with the intergrowth relationship between major gangue minerals and iron minerals.

Table 4. The results of the flash suspension roasting-magnetic separation.

Name	Yield (%)	TFe (%)		
		Grade	Recovery	Cumulative Grade
Concentrate 1	28.60	60.10	73.35	25.58
Concentrate 2	3.03	60.15	7.78	
Middling 2	7.04	10.85	3.26	
Middling1	12.82	9.44	5.16	
Tailings	48.51	5.05	10.45	
Roasted ore	100.00	23.43	100.00	

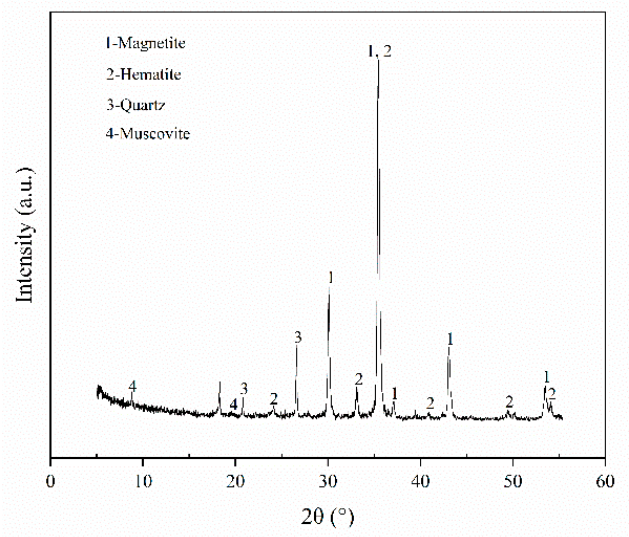

Figure 9. The XRD results of the mixed iron concentrate.

4. Conclusions

Based on the process mineralogy characteristics, the laboratory-scale recovery of iron from the discarded iron tailings using flash suspension roasting followed by magnetic separation was investigated. The MLA results show that the tailings are ground to a fineness of P90 −75 μm, where the distribution of siderite and M/H in the −75 μm particle size is 85.37% and 92.75%, respectively. Moreover, M/H and siderite are mainly associated with muscovite and quartz. This indicates that regrinding for contiguous bodies of M/H and siderite is beneficial for improving the grade and recovery of iron concentrates. Therefore, with the suspension roasting conditions, comprising a milled tailing fineness of P90 −75 μm, the roasting time of 3–4 s, the reductant dosage of 10% CO in the CO_2, the roasting temperature of 780 °C, a mixed iron concentrate containing 60.10% Fe with an iron recovery of 81.13% would be achieved after selective grinding and staged magnetic separation of the roasted ore. The result indicates that the flash suspension roasting effects with 3–4 s roasting time are achievable; the regrinding process of the middling can help to improve the recovery of iron concentrates. The study provides an efficient approach for recovering refractory iron from tailings.

Supplementary Materials: The following supporting information can be downloaded at: https://www.mdpi.com/article/10.3390/min12060676/s1, Figure S1: Schematic diagram of the flash suspension reactor.

Author Contributions: Conceptualization, H.W. and X.B.; methodology, H.W., P.Y. and J.Q.; formal analysis, P.Y. and C.Z.; investigation, H.W., J.Q. and X.B.; resources, C.Z.; data curation, H.W. and J.Q.; writing—original draft preparation, H.W. and J.Q.; writing—review and editing, S.L. and S.Y.; supervision, X.B.; project administration, X.B.; funding acquisition, H.W. and X.B. All authors have read and agreed to the published version of the manuscript.

Funding: This research was funded by Shaanxi Provincial Natural Science Basic Research Program (Grant No. 2019JLZ-05), Shaanxi Provincial Department of Education Service Local Special Project (Grant No.21JC021), China Scholarship Council (Grant No. 202008610058), National Natural Science Foundation of China (Grant No. 51904222), Shaanxi International Cooperation and Exchange Project (Grant No. 2021KWZ-16), Xi'an University of Architecture and Technology Special Project for Natural Science (Grant No. ZR20066) and the Natural Science Foundation of Qinghai Province, China (Grant No. 2021-ZJ-975Q).

Institutional Review Board Statement: Not applicable.

Informed Consent Statement: Not applicable.

Data Availability Statement: All data, models, and code generated or used during the study appear in the article.

Acknowledgments: The authors are grateful to Yanxin Chen, Shaowu Jiu, and Chao Yang for providing the flash suspension roasting experiment and funding support.

Conflicts of Interest: The authors declare no conflict of interest.

References

1. Florén, H.; Frishammar, J.; Löf, A.; Ericsson, M. Raw materials management in iron and steelmaking firms. *Miner. Econ.* **2019**, *32*, 39–47. [CrossRef]
2. Cen, P.; Bian, X.; Liu, Z.; Gu, M.; Wu, W.; Li, B. Extraction of rare earths from bastnaesite concentrates: A critical review and perspective for the future. *Miner. Eng.* **2021**, *171*, 107081. [CrossRef]
3. Fijorek, K.; Jurkowska, A.; Jonek-Kowalska, I. Financial contagion between the financial and the mining industries–Empirical evidence based on the symmetric and asymmetric CoVaR approach. *Resour. Policy* **2021**, *70*, 101965. [CrossRef]
4. Mishra, D.P.; Swain, S.K. Global trends in reserves, production and utilization of iron ore and its sustainability with special emphasis to India. *J. Mines Met. Fuels* **2020**, *68*, 11–18.
5. Roy, S.K.; Nayak, D.; Rath, S.S. A review on the enrichment of iron values of low-grade Iron ore resources using reduction roasting-magnetic separation. *Powder Technol.* **2020**, *367*, 796–808. [CrossRef]
6. Yu, J.; Han, Y.; Li, Y.; Gao, P. Recent advances in magnetization roasting of refractory iron ores: A technological review in the past decade. *Miner. Process. Extr. Metall. Rev.* **2020**, *41*, 349–359. [CrossRef]
7. Tang, Z.; Gao, P.; Han, Y.; Guo, W. Fluidized bed roasting technology in iron ores dressing in China: A review on equipment development and application prospect. *J. Miner. Metall. B* **2019**, *55*, 295–303. [CrossRef]
8. Sun, Y.; Zhang, X.; Han, Y.; Li, Y. A new approach for recovering iron from iron ore tailings using suspension magnetization roasting: A pilot-scale study. *Powder Technol.* **2020**, *361*, 571–580. [CrossRef]
9. Sun, Y.; Zhu, X.; Han, Y.; Li, Y. Green magnetization roasting technology for refractory iron ore using siderite as a reductant. *J. Clean. Prod.* **2019**, *206*, 40–50. [CrossRef]
10. Zhang, Q.; Sun, Y.; Han, Y.; Li, Y.; Gao, P. Producing magnetite concentrate via self-magnetization roasting in N2 atmosphere: Phase and structure transformation, and extraction kinetics. *J. Ind. Eng. Chem.* **2021**, *104*, 571–581. [CrossRef]
11. Zhang, Q.; Sun, Y.; Han, Y.; Gao, P.; Li, Y. Thermal Decomposition Kinetics of Siderite Ore during Magnetization Roasting. *Min. Metall. Explor.* **2021**, *38*, 1497–1508. [CrossRef]
12. Zhang, Q.; Sun, Y.; Han, Y.; Li, Y. Pyrolysis behavior of a green and clean reductant for suspension magnetization roasting. *J. Clean. Prod.* **2020**, *268*, 122173. [CrossRef]
13. Zhang, X.; Han, Y.; Li, Y.; Sun, Y. Effect of heating rate on pyrolysis behavior and kinetic characteristics of siderite. *Minerals* **2017**, *7*, 211. [CrossRef]
14. Zhang, Q.; Sun, Y.; Han, Y. Research on Kinetics of FeO Magnetization Reaction in the Thermal Decomposition of Siderite. *Met. Mine* **2019**, *48*, 50.
15. Feng, Z.; Yu, Y.; Liu, G.; Chen, W. Thermal decomposition kinetics of siderite in nitrogen. *J. Wuhan Univ. Technol.* **2009**, *31*, 11–14.
16. Yuan, S.; Zhou, W.; Han, Y.; Li, Y. Efficient enrichment of low-grade refractory rhodochrosite by preconcentration-neutral suspension roasting-magnetic separation process. *Powder Technol.* **2020**, *361*, 529–539. [CrossRef]

17. Yuan, S.; Zhou, W.; Han, Y.; Li, Y. Individual enrichment of manganese and iron from complex refractory ferromanganese ore by suspension magnetization roasting and magnetic separation. *Powder Technol.* **2020**, *373*, 689–701. [CrossRef]
18. Liu, J.; Nie, Q.; Han, Y. Effect of particle size of suspension roasting of oolitic hematite. *J. China Univ. Min. Technol.* **2018**, *2*, 415–420. (In Chinese)
19. Gao, P.; An, Y.; Li, G.; Han, Y. Effect of particle size on reduction kinetics of hematite ore in suspension roaster. *Physicochem. Probl. Miner. Processing* **2020**, *56*, 449–459. [CrossRef]
20. Jiao, Y.; Qiu, K.H.; Zhang, P.C.; Li, J.F.; Zhang, W.T.; Chen, X.F. Process mineralogy of Dalucao rare earth ore and design of beneficiation process based on AMICS. *Rare Met.* **2020**, *39*, 959–966. [CrossRef]
21. Hu, W.; Tian, K.; Zhang, Z.; Guo, J.; Liu, X.; Yu, H.; Wang, H. Flotation and Tailing Discarding of Copper Cobalt Sulfide Ores Based on the Process Mineralogy Characteristics. *Minerals* **2021**, *11*, 1078. [CrossRef]
22. Xu, W.; Shi, B.; Tian, Y.; Chen, Y.; Li, S.; Cheng, Q.; Mei, G. Process Mineralogy Characteristics and Flotation Application of a Refractory Collophanite fromGuizhou, China. *Minerals* **2021**, *11*, 1249. [CrossRef]
23. Qu, S. Process mineralogy of an iron ore from Daxigou. *Min. Met. Eng.* **2019**, *39*, 70–72.
24. Gu, Y. Automated scanning electron microscope based mineral liberation analysis an introduction to JKMRC/FEI mineral liberation analyser. *J. Miner. Mater. Charact. Eng.* **2003**, *2*, 33–41. [CrossRef]
25. Fandrich, R.; Gu, Y.; Burrows, D.; Moeller, K. Modern SEM-Based Mineral Liberation Analysis. *Inter. J. Miner. Process.* **2007**, *84*, 310–320. [CrossRef]
26. Sandmann, D. Use of mineral liberation analysis (MLA) in the characterization of lithium-bearing micas. *J. Miner. Mater. Character. Eng.* **2013**, *1*, 285. [CrossRef]
27. Schulz, B.; Merker, G.; Gutzmer, J. Automated SEM mineral liberation analysis (MLA) with generically labelled EDX spectra in the mineral processing of rare earth element ores. *Minerals* **2019**, *9*, 527. [CrossRef]
28. Jin, J.; Zhou, W.; Sun, Y.; Han, Y.; Li, Y. Reaction Characteristics and Existing Form of Phosphorus during Coal-Based Reduction of Oolitic Iron Ore. *Minerals* **2021**, *11*, 247. [CrossRef]
29. Guo, X.; Ren, W.; Zhang, M.; Dai, S.; Zhao, T.; Zhu, J. Effects of grinding fineness on magnetism and agglomeration of magnetite. *J. Cent. South Univ. Sci. Technol.* **2020**, *51*, 2373–2378. (In Chinese)
30. Li, L.; Sheng, S.; Yuan, Z. Loss mechanism of fine-grained ilmenite in magnetic separation. *China Mine* **2018**, *27*, 138–144. (In Chinese)
31. Zhang, X.; Han, Y.; Li, Y.; Tang, Z. New Process of Comprehensive Utilization for Daxigou Refractory Siderite Ore. *J. Northeast. Univ. Nat. Sci.* **2018**, *39*, 248.
32. Li, Y.; Sun, T.; Zou, A.; Xu, C. Effect of coal levels during direct reduction roasting of high phosphorus oolitic hematite ore in a tunnel kiln. *Int. J. Min. Sci. Technol.* **2012**, *22*, 323–328. [CrossRef]
33. Zhang, X.; Han, Y.; Sun, Y.; Li, Y. Innovative utilization of refractory iron ore via suspension magnetization roasting: A pilot-scale study. *Powder Technol.* **2019**, *352*, 16–24. [CrossRef]